

# Thickness effect on fracture in high impact polystyrene

O. F. YAP, Y. W. MAI, B. COTTERELL

*Department of Mechanical Engineering, University of Sydney, Sydney, New South Wales 2006, Australia*

The effect of thickness on the fracture behaviour of a high-impact polystyrene containing approximately 7% rubber is studied. For thicknesses below 10 mm plane stress ductile tearing occurs and deep edge notched tension specimens are used to obtain the specific essential work of fracture ( $w_e$ ) in plane strain. Mixed mode plane strain-plane stress fracture is predominant in single-edge notched tension specimens with thicknesses above 10 mm. By assuming that the plane stress layers are given by the overall fracture toughness ( $K_c$ ) a modified bimodal fracture analysis based on linear elastic fracture mechanics concepts is presented to analyse the experimental results. The plane strain fracture toughness  $G_{c1}$  ( $= K_{c1}^2/E$ ) is in good agreement with  $w_e$ . It is shown that  $K_{c1}$  for HIPS is larger than that of the polystyrene matrix alone due to the toughening effect of the rubber at the crack tip vicinity.

## 1. Introduction

Many polymeric materials, such as the polyolefines, polyamides and rubber-toughened styrenes, have been increasingly used in a large variety of engineering applications where previously only metals were employed. These polymers are normally ductile and tough when tested in the laboratory using small size samples. However, in field services brittle fractures have occurred in these materials. Birch *et al.* [1] have discussed a range of potential factors that can cause a ductile polymer to behave in a brittle manner. These include fatigue loading; low temperatures [2]; high strain rates such as experienced in impact tests [3]; environmental attack, both liquid and gaseous [3, 4]; presence of internal flaws and surface scratches; and thick sections. These factors can either operate independently or jointly in combinations. For design against catastrophic brittle fracture it is necessary to determine the plane strain fracture toughness ( $K_{c1}$ ) of the polymer. However, the determination of valid  $K_{c1}$  values for ductile polymers with large fracture toughness and low yield-strength ratios requires enormously thick specimens which are difficult to obtain. As suggested by Fernando and

Williams [5], in order to overcome these difficulties, alternative test techniques may be developed to provide some constraints to plastic flow so that brittle fracture is encouraged. For example, surface notches with sharp root radius ( $\leq 25 \mu\text{m}$ ) or fatigue precracks [2, 5] have been shown to produce brittle fracture in polymers with such thicknesses that would otherwise only give ductile tearing. The bending mode is preferred to the tension mode because of the slightly larger plastic constraint [6].

In a previous paper [7] we have investigated several ways of promoting brittle fracture in a high-impact polystyrene with approximately 7% rubber content. One such method is based on the model given by Atkins and Mai [8] whereby the high-impact polystyrene (HIPS) layer is sandwiched with two outside epoxy resin layers. The epoxy resin layers provide enhanced constraint to the HIPS so that its effective yield stress is raised, crazing is suppressed, and brittle fracture is promoted. The analysis according to Mai and co-workers [7, 8] gives a brittle fracture toughness of  $1.74 \text{ MPa m}^{1/2}$  for HIPS. Additional tests using surface notches and low temperatures give lower fracture toughness values indicating that the

sandwiching method has not yet imparted full plastic constraint to the HIPS in these experiments. The present paper is an extension of this previous work [7] and it examines the effect of thickness on the fracture behaviour of this same HIPS material. Depending on the size of the plastic zone relative to the thickness and the specimen in-plane dimensions a range of behaviour is expected. An understanding of this fracture behaviour and a knowledge of the thickness-dependent fracture toughness are most crucial in preventing service failures.

## 2. Experimental work

The HIPS used in the present experiments has a nominal sheet thickness of 4.7 mm. Standard tensile tests showed that the Young's modulus ( $E$ ) is 2.2 GPa, the yield strength ( $\sigma_y$ ) is 21 MPa and the ultimate elongation ( $\epsilon_f$ ) over 50 mm gauge length is  $\sim 20\%$ . Both single-edge notched (SEN) and surface notched (SN) specimens were tested in tension. Some SEN specimens were also tested in bending. The 4.7 mm thick specimens were cut to dimensions 120 mm  $\times$  300 mm. The 9.4 mm thick test pieces were 70 mm by 200 mm and the thickness was obtained by solvent bonding two 4.7 mm thick sheets face to face under pressure. Thicker specimens could not be effectively obtained by adhering multiple layers together because voids or imperfect bonding tended to form between some layers. Instead single or two-layer samples were machined with notches across the face in the flatwise direction. In this way thicknesses in the range of 20 to 120 mm could be achieved. The notch depth-to-width ratio varied from 0.16 to 0.32. In addition deep edge notched tension (DENT) specimens with thicknesses 4.7 and 9.4 mm were prepared to sizes 70 mm  $\times$  200 mm for the plane stress ductile fracture experiments. The ligament length varied from 2 to 17 mm. The notches in all the SEN, SN and DENT specimens were machined at room temperature with a sharp fly cutter having a tip radius of  $\sim 20 \mu\text{m}$ . All fracture experiments were conducted in an Instron testing machine with a nominal strain rate of  $5 \times 10^{-3} \text{ sec}^{-1}$  at a temperature of  $23 \pm 2^\circ \text{C}$  and a relative humidity of  $55 \pm 2\%$ .

The brittle fracture toughness ( $K_c$ ) at instability is related to the fracture stress ( $\sigma_c$ ) and the crack length ( $a$ ) by:

$$K_c = \sigma_c Y a^{1/2}, \quad (1)$$

where  $Y$  is a geometric factor being a function of crack length and loading configurations [9–11]. For this equation to be valid the plastic zone size,

$$r_p = \frac{1}{2\pi} \left( \frac{K_c}{\sigma_y} \right)^2,$$

must be small compared to the initial crack length and the other in-plane dimensions. In the case of limited plasticity,  $r_p$  can be added to  $a$  in Equation 1 to calculate  $K_c$  by an iterative procedure.

## 3. Thickness effect on fracture

There is a substantial thickness effect on the fracture behaviour of HIPS as shown in Fig. 1. Above 40 mm  $K_c$  is independent of thickness and notch geometry with a value of  $\sim 1.45 \text{ MPa m}^{1/2}$  indicating that this is, in fact, the plane strain fracture toughness ( $K_{c1}$ ) for the HIPS. The fractures are completely brittle. It is apparent from these experimental results that the minimum thickness ( $B$ ) required by the ASTM Standards for plane strain conditions,  $B \geq 2.5(K_c/\sigma_y)^2$ , is insufficient for this material and that at least three times the recommended thickness is needed. For the SN tension specimens the data of which are plotted on apparent thicknesses [2, 5, 15], the thickness required can be smaller with  $B \geq 5(K_{c1}/\sigma_y)^2$ . Between 10 and 40 mm,  $K_c$  decreases with increasing thickness. The fracture is a mixed plane strain–plane stress mode which is accompanied by small-scale yielding at the crack tip. The SEN specimens in tension were all unstable but it was not possible to promote unstable cracking for the SEN specimens in bending even though the plastic constraint factor is larger [6]. The conditions governing the stability of cracking are likely to be more significant in these fracture experiments [12]. For thicknesses below 10 mm, valid  $K_c$  values are difficult to obtain with the specimen size used. The plastic zone size is larger than the specimen thickness and is of the order of the initial crack lengths. There is also a considerable amount of slow crack growth or ductile tearing before an instability is reached. Linear elastic fracture mechanics (LEFM) concepts such as that of Equation 1 are inapplicable to the analysis of this type of fracture.

## 4. Bimodal fracture analysis

### 4.1. The model-partition of $K$ and $G$

The dependence of fracture toughness on thick-

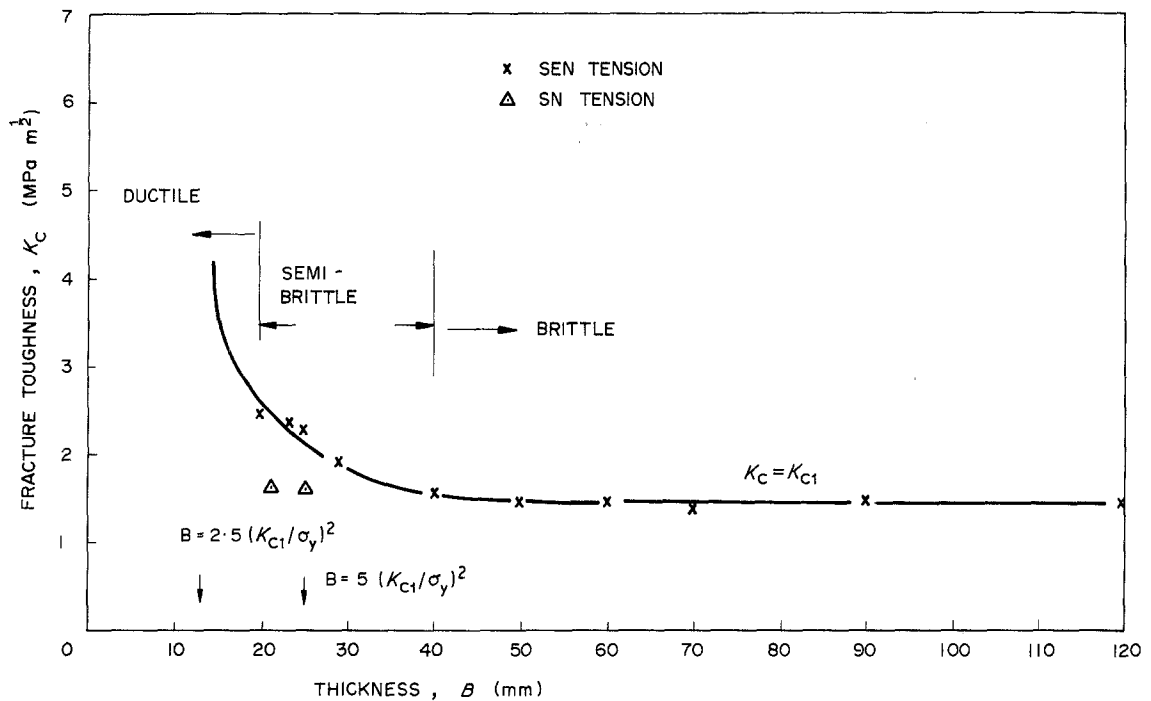


Figure 1 Variation of fracture toughness ( $K_c$ ) with thickness ( $B$ ).

ness can be modelled by a bimodal fracture analysis [2, 5, 7, 8, 13–20]. The fracture is assumed to be plane strain in the mid-thickness which is sandwiched between two external layers in plane stress each with width  $r_p$ . The total fracture toughness ( $K_c$ ) measured, thus consists of two contributions: one by the plane strain strip ( $K_{c1}$ ) and the other the plane stress layers ( $K_{c2}$ ). By partitioning  $K_c$  into  $K_{c1}$  and  $K_{c2}$  according to thickness proportions it can be shown that:

$$K_c = K_{c1} \left(1 - \frac{2r_p}{B}\right) + K_{c2} (2r_p/B) \quad (2)$$

It is claimed that this equation gives a good description of the thickness-dependent fracture behaviour of a wide range of ductile polymers [2, 5, 15–17]. Recently, Guild *et al.* [18] and Atkins [19] have argued that the  $K$ -partitioning method is merely load-sharing between the layers and that shear stress transfer between adjacent layers cannot be ignored as in Equation 2. They suggest that the partitioning of strain energy release rates is more appropriate. Thus,\*

$$G_c = G_{c1} \left(1 - \frac{2r_p}{B}\right) + G_{c2} (2r_p/B) \quad (3)$$

\*In Guild *et al.* [18],  $2r_p$  is the thickness of the PVC and  $(B - 2r_p)$  is that for PMMA.

where the subscripts for  $G$  have the same meaning as for  $K$ . Guild *et al.* [18] have provided a statistical analysis of their experimental data to support that Equation 3 is better than Equation 2 in predicting the thickness dependence of fracture toughness. Fraser and Ward [13] also use Equation 3 to analyse their experimental results for polycarbonate. The difference between these two approaches can be compared as follows. In terms of  $K$ , equation 3 is rewritten as:

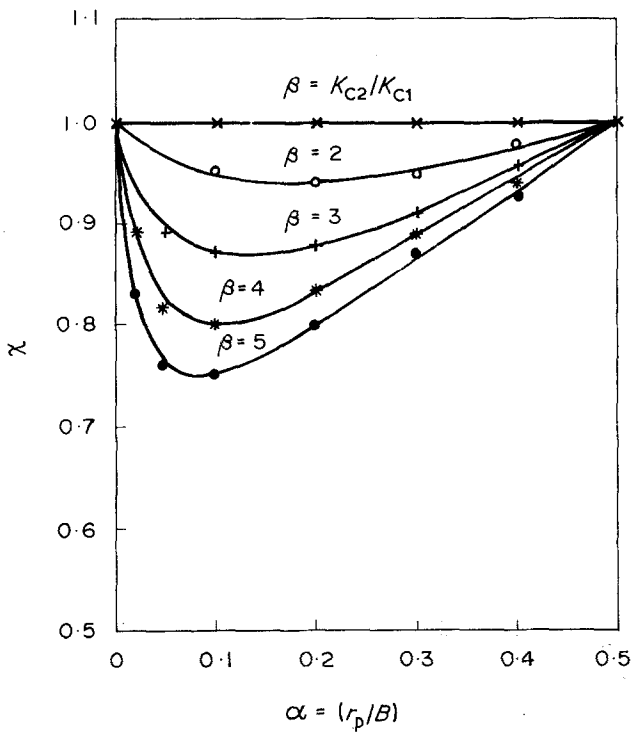
$$K_c = \left[ K_{c1}^2 \left(1 - \frac{2r_p}{B}\right) + K_{c2}^2 (2r_p/B) \right]^{1/2} \quad (4)$$

If  $\chi$  defines the ratio of Equation 3 to Equation 4, i.e. the arithmetic mean as opposed to the root mean square, then

$$\chi = \frac{(1 - 2\alpha) + 2\alpha\beta}{[(1 - 2\alpha) + 2\alpha\beta^2]^{1/2}} \quad (5)$$

where  $\alpha = r_p/B$  and  $\beta = K_{c2}/K_{c1}$ . Fig. 2 shows how  $\chi$  varies with  $\alpha$  for different  $\beta$ . When  $\alpha = 0$  the fracture is completely plane strain and when  $\alpha = 0.5$  it is all plane stress. For many polymers  $\beta \leq 3$  so that for practical purposes the two approaches to the bimodal fracture analysis do not yield widely different results. The maximum

Figure 2 Variation of  $\chi$  with  $\alpha$  for varying  $\beta$ .



difference for  $\alpha = 0.1$  and  $\beta = 3$  is only 13%. In the present work, however, the energy partition approach is followed for the same reasons stated in our previous paper [7]. This approach is the same as that originally suggested for metals [20–22].

#### 4.2. Width of shear lip and plane stress layer

In the bimodal fracture analysis the plane stress layers on the outside are subjected to shear yielding giving rise to the formation of shear lips. In metals it is usual to equate this shear lip width ( $w$ ) to the thickness of the plane stress layers. Theoretical estimate of the lip width is difficult because little is known about the specific details of the change of plane stress to plane strain across the thickness. The increase of lip width with slow crack growth [22] adds further complexity to the problem. It is usually assumed in metals that the shear lip width is constant and is given by [20–22]:

$$w = r_{p1} = \left( \frac{EG_{c1}}{\sigma_y^2} \right) = \frac{1}{2\pi} \left( \frac{K_{c1}}{\sigma_y} \right)^2 \quad (6)$$

where the plane strain fracture toughness values,  $G_{c1}$  and  $K_{c1}$ , are used. Although shear lips are known to form in some polymers [13–15] this is

not a necessary condition for the bimodal fracture analysis. For example, HIPS does not have shear lips but the thickness effect on  $K_c$  is apparent in Fig. 1 [15, 16]. It has been suggested [15–17] that for polymers the plane stress toughness ( $K_{c2}$ ) is associated with bulk yielding or full effects of crazing (such as in rubber-toughened polymers) and that the width of the plane stress layers is given by the penetration of the plane stress plastic zone size ( $r_{p2}$ ), i.e.

$$r_{p2} = \frac{1}{2\pi} \left( \frac{K_{c2}}{\sigma_y} \right)^2 \quad (7)$$

Equation 7 clearly predicts a much thicker plane stress layer than Equation 6 since  $K_{c2} > K_{c1}$ . A search of the literature casts some doubts on the accuracy of these two equations to estimate  $r_{p1}$  or  $r_{p2}$ . Bluhm [20] claimed that the shear lip width is a constant in metals but this has been completely refuted by the work of De Sisto *et al.* [23] who showed that  $w$  varies with  $B$ . It is not possible to determine the variation of  $w$  with  $K_c$  from this work [23] because not all the  $K_c$  values reported are valid. However, for large thicknesses satisfying the plane strain conditions  $w$  tends to a limiting value given by Equation 6. There is evidence from the results of a high-strength maraging steel (Fig. 4.9, p. 101

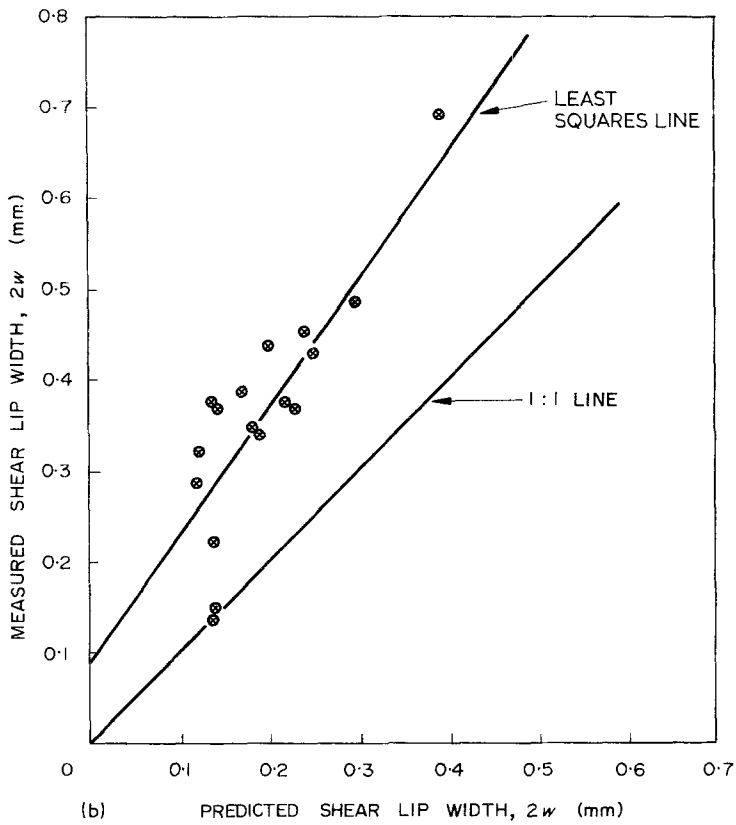
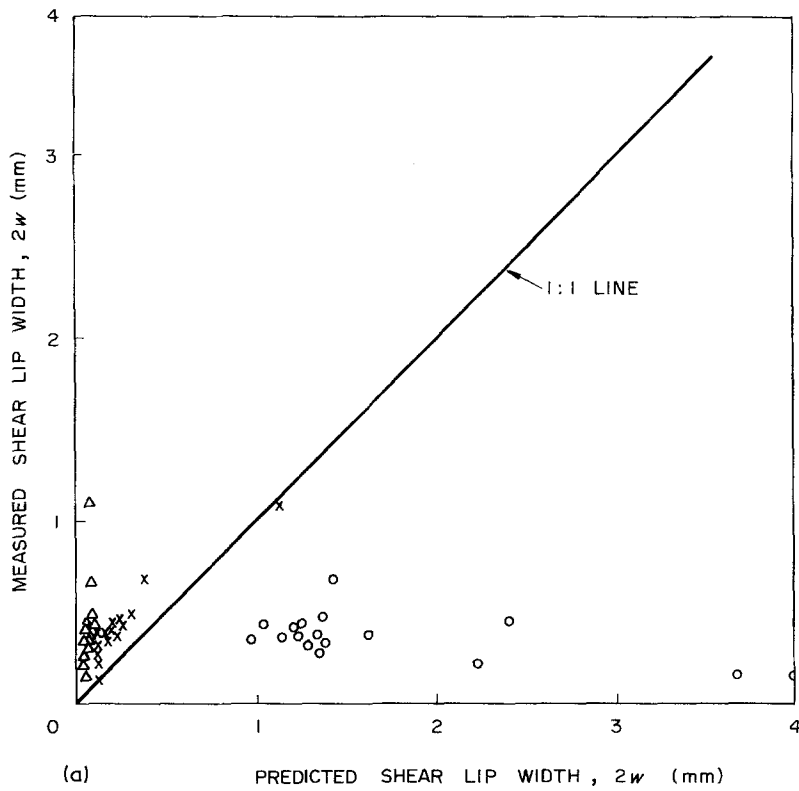


Figure 3 A comparison of experimental and theoretical shear lip widths ( $w$ ) for PC at  $-20^{\circ}\text{C}$ . (a) Theoretical values based on  $K_{c1}$ ,  $K_{c2}$  and  $K_c$ ; (b) enlarged scale for theoretical values based on  $K_c$ .  $\Delta r_{p1}$ ,  $\circ r_{p2}$ ,  $\times r_p$ . (After Fraser and Ward [13].)

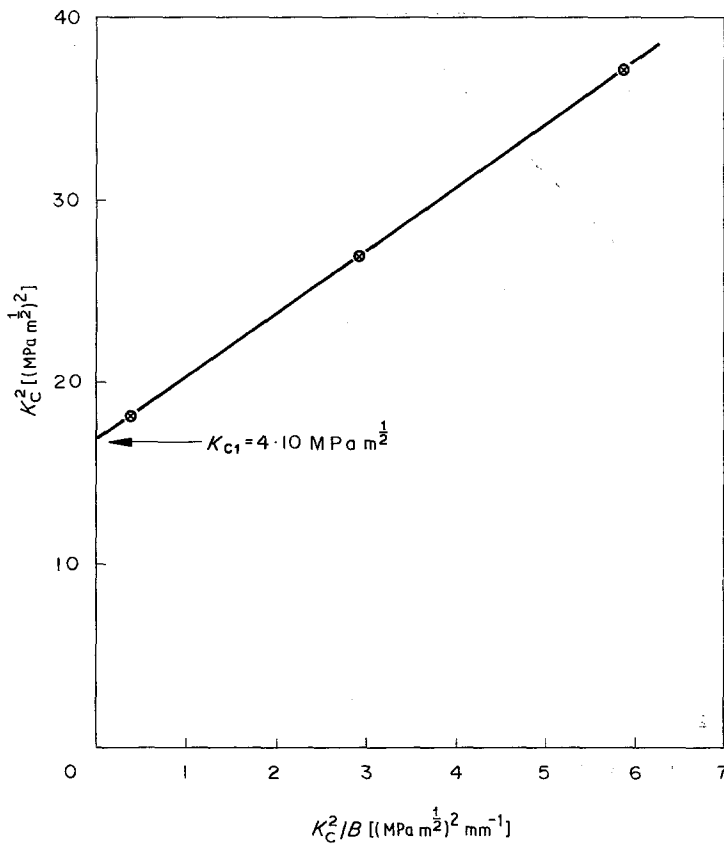


Figure 4 A plot of  $K_c^2$  against  $(K_c^2/B)$  for PP according to Equation 9.

of [24]) to suggest that  $w$  increases as  $K_c$  increases. In polymers such as polycarbonate and polypropylene [2, 5, 15] Equation 7 grossly overestimates the actual  $r_{p2}$  measurements. By replacing  $K_{c2}$  with  $K_c$ , the thickness-dependent fracture toughness, the predicted  $r_{p2}$  for the polycarbonate studied in [15] is approximately 0.1 mm for all temperatures below  $-60^\circ\text{C}$ . This predicted value is in much better agreement with the experimental results. Based on these experimental observations it is reasonable to propose that the width of the shear slip and of the plane stress layer is given by the overall fracture toughness,  $K_c$  or  $G_c$ , i.e.

$$r_p = \frac{1}{2\pi} \left( \frac{K_c}{\sigma_y} \right)^2 = \frac{1}{2\pi} \left( \frac{EG_c}{\sigma_y^2} \right). \quad (8)$$

This obviously means that  $r_p$  is thickness dependent as  $K_c$  and  $G_c$  vary with thickness. The extensive experimental data on polycarbonate taken from Fraser and Ward [13] and replotted in Fig. 3a and b give some further support that Equation 8 is better than either Equation 6 or 7 in predicting the shear lip width or the plane stress layer thickness.

Combining Equations 3, 4 and 8 it can be

shown that the overall fracture toughnesses are given by:

$$K_c^2 = K_{c2} + \left( \frac{K_c}{\sigma_y} \right)^2 \frac{1}{\pi B} (K_{c2}^2 - K_{c1}^2) \quad (9)$$

and

$$G_c = G_{c1} + \left( \frac{EG_c}{\sigma_y^2} \right) \frac{1}{B\pi} (G_{c2} - G_{c1}). \quad (10)$$

where  $B \rightarrow \infty$ ,  $K_c = K_{c1}$  and  $G_c = G_{c1}$ ; when  $B = 2r_p$ ,  $K_c = K_{c2}$  and  $G_c = G_{c2}$ . Since  $(K_{c1}, K_{c2})$  and  $(G_{c1}, G_{c2})$  are material properties and if they are known or predetermined from separate experiments the thickness-dependent fracture toughness ( $K_c, G_c$ ) can be predicted easily from Equations 9 and 10, i.e.

$$K_c^2 = K_{c1}^2 / \left[ 1 - \left( \frac{K_{c2}^2 - K_{c1}^2}{\sigma_y^2 \pi B} \right) \right] \quad (11)$$

and

$$G_c = G_{c1} / \left\{ 1 - \left[ \frac{(G_{c2} - G_{c1})E}{\pi B \sigma_y^2} \right] \right\}. \quad (12)$$

The polypropylene and polycarbonate data taken from the work of Williams and co-workers [5, 15] are replotted according to Equation 9 in Figs 4 and 5. As predicted, a straight-line relationship

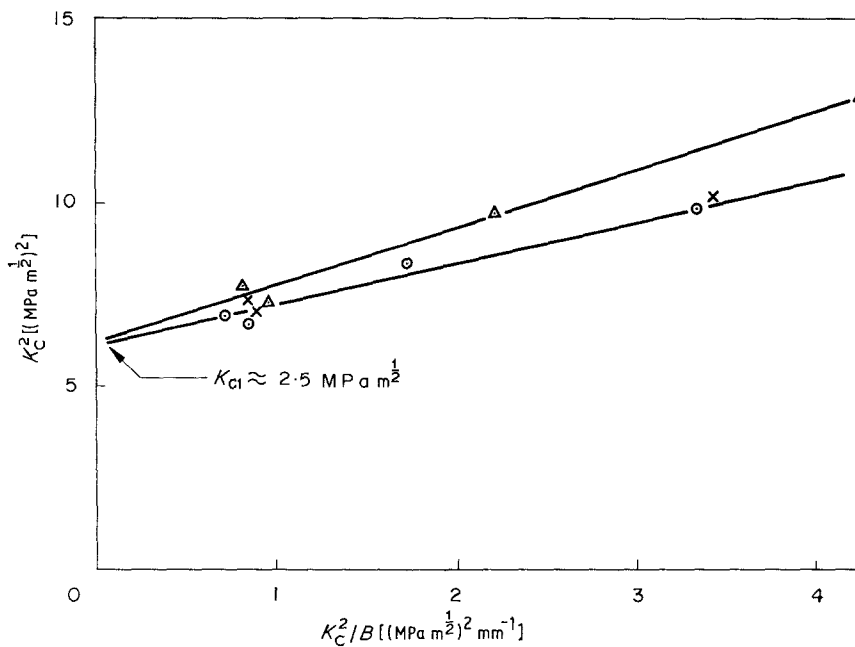


Figure 5 A plot of  $K_c^2$  against  $(K_c^2/B)$  for PC according to Equation 9. x  $0^\circ\text{C}$ , o  $-40^\circ\text{C}$ , Δ  $100^\circ\text{C}$ .

is obtained between  $K_c^2$  and  $(K_c^2/B)$ . The intercepts give  $K_{c1} = 4.10\text{ MPa m}^{1/2}$  for PP and  $2.50\text{ MPa m}^{1/2}$  for PC for the three temperatures. These results are in excellent agreement with those obtained by Williams and co-workers [5, 15] using Equation 2. The slopes of the lines give  $K_{c2} = 8.10\text{ MPa m}^{1/2}$  for PP and  $4.83\text{ MPa m}^{1/2}$  ( $0^\circ\text{C}$ ),  $5.88\text{ MPa m}^{1/2}$  ( $-40^\circ\text{C}$ ) and  $8.84\text{ MPa m}^{1/2}$  ( $-100^\circ\text{C}$ ) for PC. These should be compared

with the corresponding values given previously [5, 15], i.e.  $7.40\text{ MPa m}^{1/2}$  for PP and  $5.00$ ,  $5.50$  and  $7.00\text{ MPa m}^{1/2}$  respectively for PC. The experimental results for PC of Fraser and Ward [13] can also be replotted according to Equation 10 as shown in Fig. 6. There is a linear relationship between  $G_c$  and  $(G_c/B)$  and this gives  $G_{c1} = 1.05\text{ KJ m}^{-2}$  and  $G_{c2} = 23.8\text{ KJ m}^{-2}$ . Fraser and Ward plotted their results according to

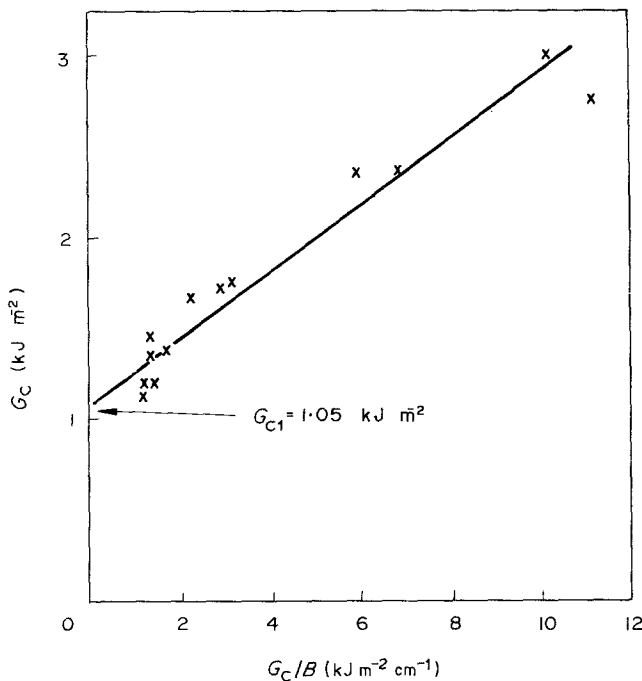


Figure 6 A plot of  $G_c$  against  $(G_c/B)$  for PC at  $-20^\circ\text{C}$  according to Equation 10.

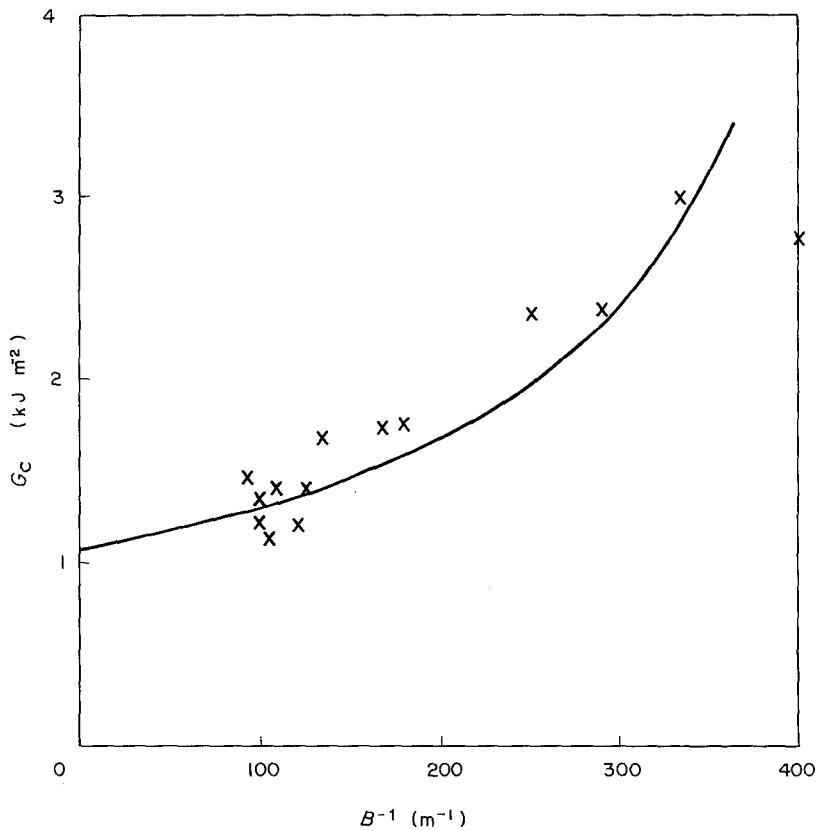


Figure 7 Variation of  $G_c$  with  $B^{-1}$  for PC at  $-20^\circ\text{C}$ . Solid curve is predicted from Equation 12 with  $G_{c1} = 1.05\text{ KJ m}^{-2}$ ,  $G_{c2} = 23.8\text{ KJ m}^{-2}$ ,  $E = 2.89\text{ GPa}$  and  $\sigma_y = 105\text{ MPa}$  [13].

Equation 3 with a constant  $r_p$  so that  $G_c$  rises linearly with  $(1/B)$ . However, it seems that their data can be equally well described by Equation 12 as given in Fig. 7. This is suggested to be a more accurate equation as  $G_c$  should tend to  $G_{c1}$  asymptotically with increasing thickness.

Equations 9 to 12 can also be used to analyse the thickness-dependent fracture toughness of metals, e.g. the high-strength maraging steel data given in Fig. 4.8, p. 100 of [24]. However, these results will not be shown here.

### 4.3. Analysis of HIPS results

The fracture toughness ( $K_c$ ) for SEN tension specimens with thicknesses larger than 10mm is plotted against  $(1/B)$  in Fig. 8 according to Equation 2. The least squares line shows that when  $B \rightarrow \infty$ ,  $K_{c1} = 1.05\text{ MPa m}^{1/2}$  which is the styrene matrix value. This seems to support the  $K_{c1}$  assumption made in previous studies on rubber-modified polystyrenes [15, 16]. However, a detailed examination of these results show that  $K_c$  tends to a constant value of  $1.45\text{ MPa m}^{1/2}$  for

$B$  larger than 40mm. The crack initiation data all give excellent agreement with this value so that  $K_{c1} = 1.45\text{ MPa m}^{1/2}$ . It is not unexpected that under full plane strain conditions HIPS can have a  $K_{c1}$  value larger than the matrix value alone. The effect of the rubber at the crack tip region must have enhanced the toughness for crack initiation. A few additional experiments with specimens containing fatigued precracks give approximately the same  $K_{c1}$  result. It may be also noted that for ABS, another rubber-toughened polymer,  $K_{c1}$  is much larger than that of the matrix polymer [25, 26].

Fig. 9 shows the variation of  $K_c^2$  with  $B$  according to Equation 9. The least squares line drawn through all the data gives  $K_{c1} = 1.45\text{ MPa m}^{1/2}$  when  $(K_c^2/B) = 0$  and the slope gives  $K_{c2} = 4.5\text{ MPa m}^{1/2}$ . Using these toughness values and Equation 11  $K_c$  can be determined as a function of  $B$  as shown in Fig. 10. Note that now as  $B$  increases  $K_c$  tends to an asymptotic value of  $K_{c1} = 1.45\text{ MPa m}^{1/2}$ .



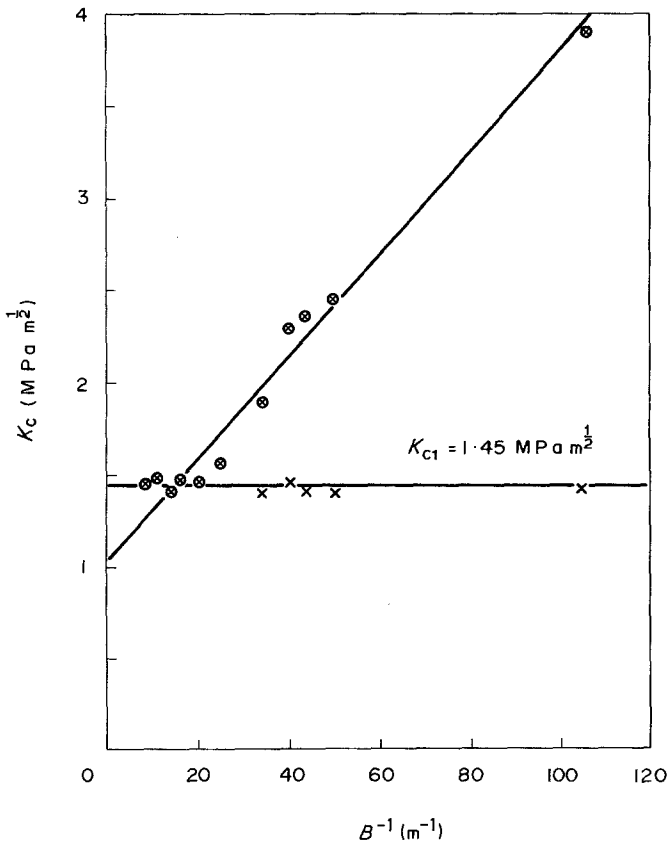


Figure 8 Variation of  $K_c$  with  $B^{-1}$  for HIPS. x crack initiation; o crack instability.

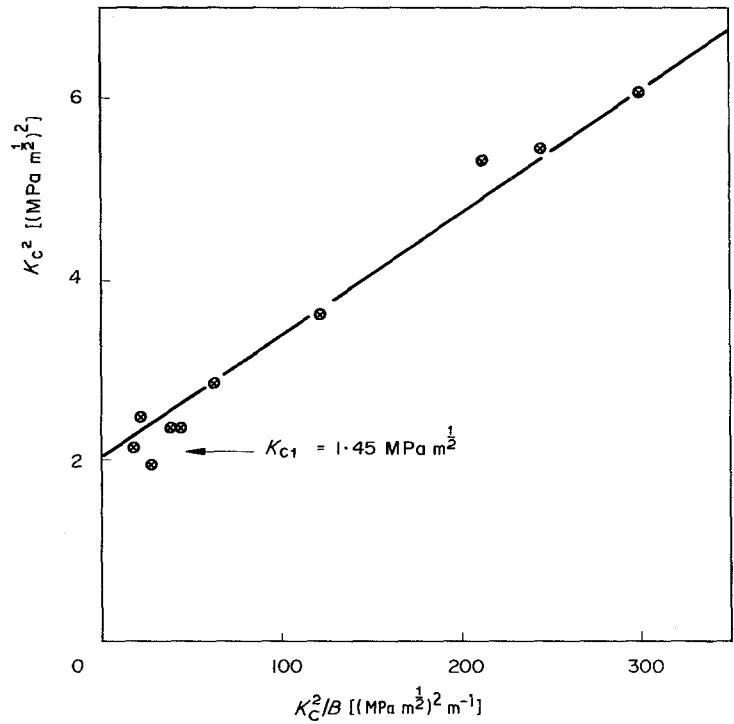


Figure 9 A plot of  $K_c^2$  against  $(K_c^2/B)$  for HIPS according to Equation 9.

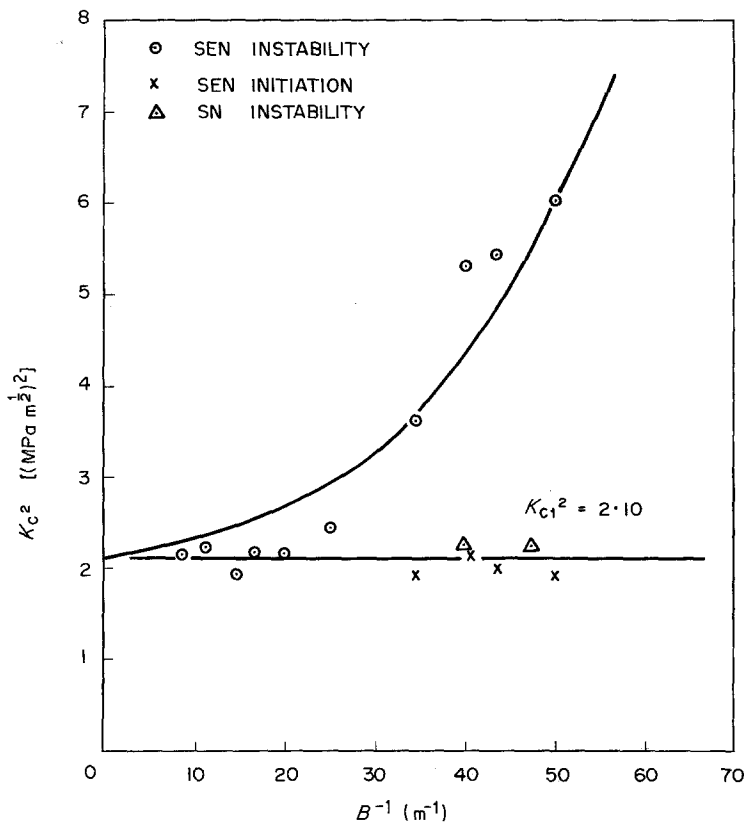


Figure 10 Variation of  $K_c^2$  with  $B^{-1}$  for HIPS. Solid curve is predicted from Equation 11 with  $K_{c1} = 1.45 \text{ MPa m}^{1/2}$ ,  $K_{c2} = 4.5 \text{ MPa m}^{1/2}$  and  $\sigma_y = 21 \text{ MPa}$ .

### 5. Plane stress ductile fracture

As discussed in Section 3, LEFM concepts cannot be applied to the SEN and SN specimens with thicknesses less than 10 mm. Post-yield fracture mechanics principles have been used in the past to analyse ductile fracture of rubber-toughened polymers in terms of both crack opening displacement and the  $J$ -integral [27–29]. The agreement with experimental results is satisfactory. In earlier work [30, 31] we have used the deep edge notched tension (DENT) specimens to study the plane stress ductile fracture behaviour of sheet metals. By plotting the total specific fracture work ( $W/lB$ ) against the ligament length ( $l$ ) and extrapolating the straight line to  $l=0$  we have obtained a specific essential work of fracture ( $w_e$ ) which is a material property being a function of thickness only.  $w_e$  is identified to  $J_p$ , the crack propagation value [31], in plane stress.

In the present work similar experiments have been performed on HIPS DENT specimens and the results given in Fig. 11. For the 4.7 mm thick specimens there is a linear relationship between ( $W/lB$ ) and  $l$  when the ligament length is less than 10 mm. For larger ligament sizes

( $W/lB$ ) is independent of  $l$ . For the thicker 9.4 mm DENT specimens we have not obtained stable cracking when  $l > 7$  mm so that only a few data are given in Fig. 11.

These results must be interpreted differently to those for metals. When the ligament length-to-thickness ratio is less than 4 for metals the fracture is suggested to be in the plane stress–plane strain transition [30] and as this ratio tends to zero the fracture tends to plane strain. The plane stress specific essential work of fracture can only be obtained with  $l/B \geq 4$ . As shown in Fig. 11 for HIPS, this plane stress–plane strain transition occurs at a smaller ratio of  $l/B = 2$ .

It is suggested here that the straight line relationship between ( $W/lB$ ) and  $l$  is partly caused by this fracture mode transition and partly because the elliptical craze zone in the ligament increases proportionally with  $l$  [32]. The least squares lines for the data of the two thicknesses give the same intercept indicating that the specific essential work of fracture ( $w_e$ ) in plane strain is independent of thickness, i.e.  $w_e = 1.10 \text{ KJ m}^{-2}$ . From Fig. 8  $K_{c1} = 1.45 \text{ MPa m}^{1/2}$  which gives  $G_{c1} = 0.96 \text{ KJ m}^{-2}$ . These results seem to indicate that  $w_e = G_{c1}$ . When  $l > 10$  mm and the plane stress

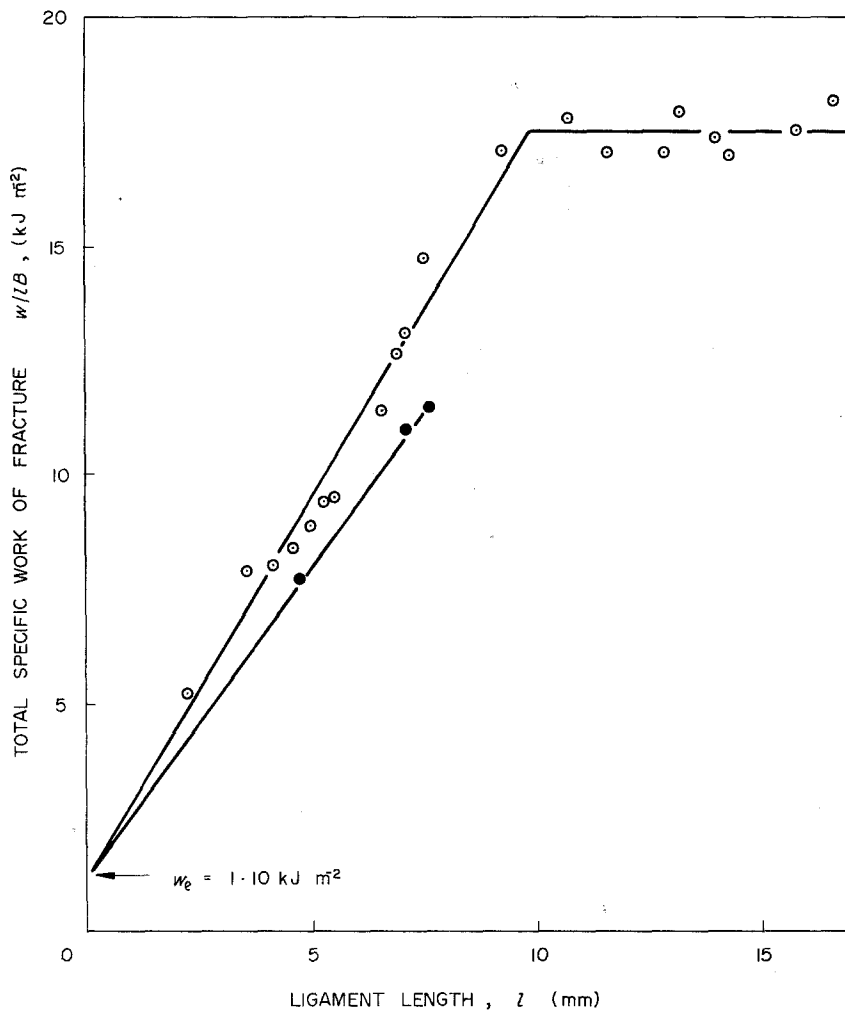


Figure 11 A plot of total specific work of fracture ( $W/lB$ ) against ligament length ( $l$ ) for HIPS.  $\circ$  4.7 mm;  $\bullet$  9.4 mm.

conditions are approached the craze zone in the ligament is changed from the elliptic geometry to a strip with a constant thickness [32]. Crack initiation occurs before the full ligament is crazed. Consequently, ( $W/lB$ ) is invariant with  $l$  as shown in Fig. 11.

Experiments on the SEN specimens show a different craze geometry at the crack tip which is identical to Fig. 17a of [27]. It is therefore likely that the plateau ( $W/lB$ ) value depends on testpiece geometry and it is not related to  $K_{c2}$  as  $w_e$  is to  $K_{c1}$ .

## 6. Conclusions

The fracture behaviour of HIPS is shown to be affected by thickness. For thicknesses bigger than 10 mm a slightly modified bimodal plane strain-plane stress fracture analysis is used to obtain the fundamental material properties,  $K_{c1}$  and

$K_{c2}$ . The width of the plane stress layers is to be given by the overall thickness-dependent toughness  $K_c$  as in Equation 8 and not by  $K_{c1}$  or  $K_{c2}$  as assumed by many previous investigators. In SEN tension specimens for  $B \geq 40$  mm  $K_c = K_{c1} = 1.45 \text{ MPa m}^{1/2}$ . This plane strain toughness is larger than the matrix due to the toughening effect provided by the rubber at crack initiation. Plane stress ductile fracture occurs in specimens with thicknesses less than 10 mm. Using deep edge notched tension specimens it is possible to obtain the plain strain essential work of fracture ( $w_e$ ) which is in good agreement with  $G_{c1}$  calculated from  $K_{c1}$ .

## References

1. M. W. BIRCH, J. G. WILLIAMS and G. P. MARSHALL, Third International Conference on Deformation, Yield and Fracture of Polymers,

- Cambridge, (The Plastics and Rubber Institute, London, 1976) pp. 6.1-6.7.
2. Y. W. MAI and J. G. WILLIAMS, *J. Mater. Sci.* **12** (1977) 1376.
  3. I. G. ZEVI, W. J. RUDIK and R. D. CORNELIUSSEN, *Polymer Eng. Sci.* **20** (1980) 622.
  4. G. P. MARSHALL, N. H. LINKINS, L. E. CULVER and J. G. WILLIAMS, *SPE J* **28** (1972) 26.
  5. P. L. FERNANDO and J. G. WILLIAMS, *Polymer Eng. Sci.* **20** (1980) 215.
  6. F. A. McCLINTOCK, *Welding J. Res. Suppl.* **26** (1961) 202-S.
  7. O. F. YAP, Y. W. MAI and B. COTTERELL, Proceedings International Conference on Analytical and Experimental Fracture Mechanics, edited by G. C. Sih and M. Mirabile (Sijthoff and Noordhoff, Netherlands, 1981) pp. 9.19-30.
  8. A. G. ATKINS and Y. W. MAI, *Int. J. Fracture* **12** (1976) 923.
  9. W. F. BROWN and J. SRAWLEY, *ASTM STP* **410** (1966).
  10. D. P. ROOKE and D. J. CARTWRIGHT, "A compendium of stress intensity factors" (HMSO, London, 1976).
  11. Y. W. MAI, *J. Testing Eval.* **6** (1978) 347.
  12. Y. W. MAI and A. G. ATKINS, *J. Strain Analysis* **15** (1980) 63.
  13. R. A. FRASER and I. M. WARD, *Polymer* **19** (1978) 220.
  14. G. L. PITMAN and I. M. WARD, *ibid.* **20** (1979) 895.
  15. M. PARVIN and J. G. WILLIAMS, *J. Mater. Sci.* **10** (1975) 1883.
  16. K. NIKPUR and J. G. WILLIAMS, *ibid.* **14** (1979) 467.
  17. M. PARVIN and J. G. WILLIAMS, *Int. J. Fracture* **11** (1975) 963.
  18. F. J. GUILD, A. G. ATKINS and B. HARRIS, *J. Mater. Sci.* **13** (1978) 2295.
  19. A. G. ATKINS, Proceedings of the Third International Conference on Mechanical Behaviour of Materials, Vol. 3, edited by K. J. Miller and R. F. Smith, (Pergamon Press, London, 1979) pp. 341-49.
  20. J. I. BLUHM, *Proc. ASTM* **61** (1961) 1324.
  21. A. S. TETELMAN and A. J. McEVILY, Jr, "Fracture of Structural Materials" (Wiley, New York, 1967).
  22. J. M. KRAFFT, A. M. SULLIVAN and R. W. BOYLE, Proceedings of the Symposium on Crack Propagation, College of Aeronautics, Cranfield, Vol. 1 (1961) 8.
  23. T. S. DeSISTO, F. L. CARR and F. R. LARSON, *Proc. ASTM* **63** (1963) 768.
  24. S. T. ROLFE and J. M. BARSOM, "Fracture and fatigue control in structures" (Prentice-Hall, New Jersey, 1977).
  25. H. J. NUSBAUM, *J. Mater. Sci.* **14** (1979) 2755.
  26. L. V. NEWMANN and J. G. WILLIAMS, *ibid.* **15** (1980) 773.
  27. R. J. FERGUSON, G. P. MARSHALL and J. G. WILLIAMS, *Polymer* **14** (1973) 451.
  28. R. D. HOFFMAN and O. RICHMOND, *J. Appl. Phys.* **47** (1976) 4289.
  29. R. D. HOFFMAN, SPE 37th Annual Technical Conference, New Orleans, (Society of Plastics Engineers, Greenwich, Conn., 1979) pp. 537-45.
  30. B. COTTERELL and J. K. REDDEL, *Int. J. Fracture* **13** (1977) 267.
  31. B. COTTERELL and Y. W. MAI, "Advances in Fracture Research", Vol. 4, edited by D. Francois, (Pergamon Press, London, 1981) pp. 1683-95.
  32. O. F. YAP, Ph. D. Thesis, University of Sydney (1982).

*Received 18 March  
and accepted 2 July 1982*